Efficient 1.3-μm electroluminescence from high concentration boron-diffused silicon p$^+$-n junctions

Invited Paper

Ting Chen (陈 挺), Guangzhao Ran (冉广照)*, Liping You (尤力平), Huabo Zhao (赵华波), and Guogang Qin (秦国刚)**

State Key Lab for Mesoscopic Physics and School of Physics, Peking University, Beijing 100871

**E-mail: rangz@pku.edu.cn; **e-mail: qingg@pku.edu.cn*

Received December 17, 2008

Electroluminescence peaking at 1.3 μm is observed from high concentration boron-diffused silicon p$^+$-n junctions. This emission is efficient at low temperature with a quantum efficiency 40 times higher than that of the band-to-band emission around 1.1 μm, but disappears at room temperature. The 1.3-μm band possibly originates from the dislocation networks lying near the junction region, which are introduced by high concentration boron diffusion.

OCIS codes: 230.3670, 260.3060, 260.3800, 130.0250.

doi: 10.3788/COL20090704.0274.

Silicon-based light sources may revolutionize telecommunications, electronics, and computing in the future[1]. Silicon-based luminescence which is completely compatible with standard Si ultra-large-scale integration (ULSI) technology has been extensively researched. Recently, researchers are more and more optimistic about silicon's light-emitting abilities. Theoretical maximal internal quantum efficiency around 20% has been predicted for silicon light-emitting diodes (LEDs)[2,3], and electroluminescence (EL) efficiency of 0.1%−1% has been achieved[4,5]. Both ion implantation[5−10]and thermal diffusion[11−14] have been used to form the p-n junctions in Si LEDs. For boron-implanted Si p-n junction, dislocation loops[5,6] or doping spikes[7,8] are used to explain the highly efficient EL and its temperature-dependent behavior. Several authors found that using silicon implantation followed by annealing to introduce dislocation loops was detrimental to the EL efficiency, and boron-diffused Si p-n junctions, which did not have those dense dislocation loops or doping spikes, had comparable or even higher EL efficiency[12−14].

The above mentioned investigations were most focused on the band-to-band emission around 1.1 μm, which would be reabsorbed easily by silicon and so was limited for applications in silicon photonics. We find an EL band around 1.3 μm from high concentration boron-diffused silicon p$^+$-n junctions. This emission is quite efficient at low temperature and its intensity is 40 times higher than that of the band-to-band emission. Through spectra measurements, electron irradiation and atomic force microscopy (AFM) observations, we show that the 1.3-μm band may originate from the dislocation networks near the junction introduced by high concentration boron diffusion.

We fabricated silicon p$^+$-n junctions by forming shallow p$^+$ region in 1 Ω·cm n-type (100) Cz-silicon wafers. The p$^+$ layer was formed by boron diffusion at 900 °C for 30 min. A 100-nm AuSb film was thermally evaporated onto the backside of the wafer, followed by rapid thermal annealing at 420 °C for 2 min, to form the cathodic ohmic contact. A semitransparent 20-nm-thick Au film was thermally evaporated onto the front surface with a mask to form 1-mm-diameter circular anode contacts. Then mesas were fabricated to avoid current leaking. A 450-nm-thick silicon layer was etched by inductively coupled plasma (ICP) etching using the front Au electrode itself as the mask. An illustration of the p$^+$-n junctions is shown in the inset of Fig. 1. Some of the samples were subjected to electron irradiation. The electron irradiation energy was 4.5 MeV and the irradiation doses were $1 \times 10^{14}, 1 \times 10^{15}$, and 1×10^{16} cm^{-2}. EL spectra were collected by a fluorescence spectrometer equipped with a Ge detector and a lock-in amplifier. The silicon p$^+$-n junctions were driven by a pulse generator (duty cycle 50% and frequency 11 Hz). AFM samples were prepared by pre-etching with Dash etchant to show the dislocation networks.

A typical current-voltage (I-V) curve is shown in Fig. 1. The forward current reaches 20 mA with the voltage of 1.1 V and the rectification ratio is higher than 10^6. The I-V characteristic confirms that the p$^+$-n junctions are well formed.

Figure 2 shows the EL spectra of the silicon p$^+$-n junctions at low temperature of 23 K (solid line) and room

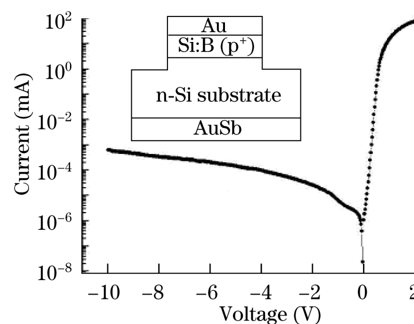

Fig. 1. Current-voltage plot for the Si p$^+$-n junction measured at room temperature. Inset shows a schematic of the Si p$^+$-n junctions. The light is emitted through the top semitransparent Au contact.

1671-7694/2009/040274-03 © 2009 Chinese Optics Letters

temperature of 295 K (dashed line). The forward current is 5 mA. The spectrum at room temperature shows only one band around 1154 nm (1.07 eV), while the spectrum at low temperature shows two bands around 1130 nm (1.10 eV) and 1295 nm (0.96 eV). The 1.07- and 1.10-eV bands were reported in many references and concluded to be the phonons assisted band-to-band emission of free carriers or free exitons in silicon[2−14]. In our experiment, the peak photon energy decreases continuously from 1.10 eV at 23 K to 1.07 eV at 295 K. For bulk crystalline Si, it is well known that the combination of thermal expansion and electron-phonon interaction contributes to the shrinkage of the band gap with increasing temperature[15]. The 1.3-μm band weakens as temperature goes up and disappears at temperatures higher than 175 K. As far as we know, in boron-diffused silicon p-n junctions, the 1.3-μm EL band is observed for the first time.

In boron-implanted silicon p-n junctions, Sun *et al.* observed two EL bands around 1.3 and 1.2 μm, and attributed them to the spatially indirect excitons bounded to doping spikes in a strained environment and without strain, respectively[7,8]. They successfully explained the abnormal temperature behavior of band-to-band emission in ion-implanted Si p-n junctions. We fabricated boron-implanted Si p-n junctions as the control samples and found the results consistent with theirs. Sobolev *et al.* also observed the 1.3-μm band in ion-implanted Si p-n junctions and attributed it to defect-related centers without further investigation of the origin[10].

To probe the origin of the 1.3-μm band, cross-sectional transmission electron microscope (XTEM) samples of boron-implanted and boron-diffused silicon p^+-n junctions were fabricated and measured. Figure 3 shows the XTEM images. For boron-implanted samples, a lot of doping spikes were observed, consistent with those reported in Refs. [7,8]. But in boron-diffused samples, although much effort was made, no similar structure was found. So we believe that the 1.3-μm band of boron-diffused silicon p^+-n junctions, though with the same wavelength as that of boron-implanted samples, does not result from doping spikes. Another obvious difference between the diffused p^+-n junctions and the implanted ones is that only the 1.3-μm band is observed in boron-diffused silicon p^+-n junctions rather than the two bands in boron-implanted samples[7,8].

Furthermore, we used electron irradiation to introduce defects into boron-diffused silicon p^+-n junctions and measured their impact on the 1.1- and 1.3-μm EL bands[16]. Figure 4 shows the EL spectra before and after electron irradiation with different doses. The inset in Fig. 4 depicts the integrated EL intensity of the two bands at different electron irradiation doses. The measurement current is 20 mA and the measurement temperature is 23 K. The intensity of the 1.1-μm band-to-band emission decreases after electron irradiation, and even decreases more than one order of magnitude after 1×10^{16} cm^{-2} electron irradiation. However, the intensity of the 1.3-μm band does not change except a slight shift of its peak wavelength.

The diffusion of high concentration substitutional impurities into shallow surface layers of silicon was found to be able to produce dislocation networks[17−21]. The reason is that the undersized substitutional impurity atoms cause strain and stress in the lattice, and when the concentration of the impurity atoms is high enough, the stress in the lattice will be relieved by formation of dislocations. Recently, several researchers used plastic deforming and direct wafer bonding to introduce dislocation networks in silicon, and observed the luminescence from dislocation networks[3,11,22]. Noticeably, their samples do not contain boron, but their photoluminescence and cathodoluminescence spectra also show 1.3-μm bands with almost the same wavelength as ours.

We used AFM to observe the dislocation networks in the high concentration boron-diffused silicon p^+-n junctions. Before AFM scan, Dash etchant was used to show the dislocation networks. The etching time was precisely controlled and the dislocation networks were proven to exist only near the junction region. In the XTEM measurement, we did not clearly observe the dislocation networks because of the limited image contrast. Figure 5 shows the AFM image of the dislocation networks in boron-diffused silicon p^+-n junctions etched to junction region. There are dense dislocation networks along the (110) direction and their areal density is about 8×10^4 cm^{-1}. It supports the conclusion that the 1.3-μm band of boron-diffused silicon p^+-n junctions originates from the dislocation networks. The emission can be

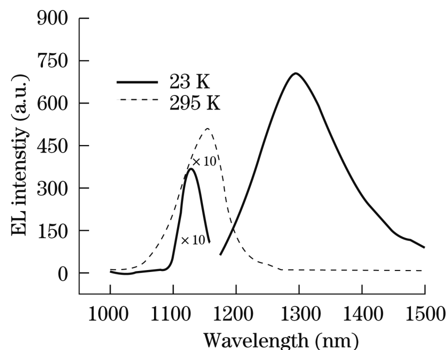

Fig. 2. EL Spectra of our boron-diffused Si p^+-n junction. The current is 5 mA.

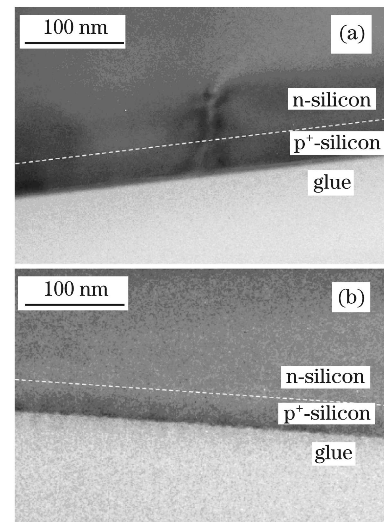

Fig. 3. XTEM images of the Si p^+-n junctions prepared by (a) boron implantation and (b) boron diffusion. The darker area is silicon.

explained by the phonon replica of the transition between the one-dimensional dislocation bands which are caused by the elastic strain field around the dislocation[22]. Because the band-to-band emission is from a relatively large region around the junction, it is easily affected by the electron irradiation. Contrastively, the dislocation networks are formed locally near the junction region, so only slight impact of electron irradiation on the 1.3-μm band can be realized. When the temperature goes up, excitons localized in dislocation networks are gradually deactivated, so the intensity of the 1.3-μm band decreases and the 1.3-μm emission disappears at room temperature[23].

In conclusion, in the high concentration boron-diffused silicon p^+-n junctions, an EL band around 1.3 μm is observed below 175 K. The 1.3-μm band is quite efficient at low temperature with a quantum efficiency 40 times higher than that of the band-to-band emission. It may originate from the dislocation networks lying near the junction region introduced by high concentration boron diffusion.

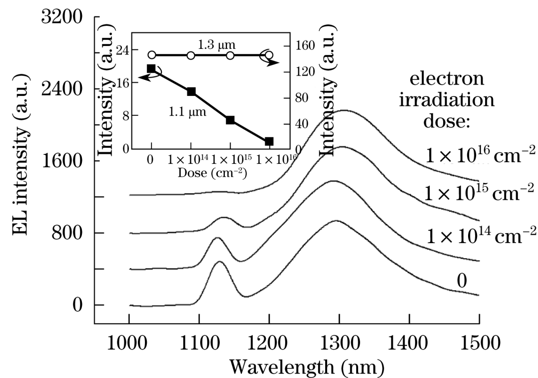

Fig. 4. EL spectra of the Si p^+-n junction before and after electron irradiation (with electron energy of 4.5 MeV and irradiation dose rate of 8.5×10^{12} $cm^{-2}s^{-1}$) of different doses ($1\times10^{14}, 1\times10^{15}$, and 1×10^{16} cm^{-2}). Inset shows the integrated EL intensities of the 1.1- and 1.3-μm bands versus electron irradiation dose. The current is 20 mA and the temperature is 23 K.

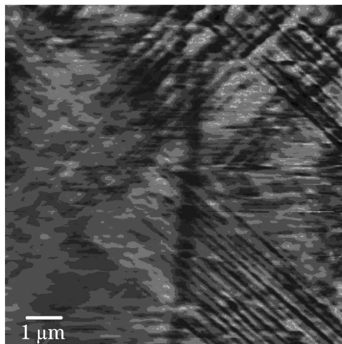

Fig. 5. AFM image of the dislocation networks in the boron-diffused silicon p^+-n junctions. The samples etched with Dash etchant show dislocation networks along (110) direction with areal density of about 8×10^4 cm^{-1}.

This work was supported by the National Natural Science Foundation of China (Nos. 10874001, 50732001, 10674012, and 60877022) and the National "973" Program of China (No. 2007CB613401).

References

1. P. Ball, Nature **409,** 974 (2001).
2. T. Trupke, J. Zhao, A. Wang, R. Corkish, and M. A. Green, Appl. Phys. Lett. **82,** 2996 (2003).
3. M. Kittler, M. Reiche, T. Arguirov, W. Seifert, and X. Yu, Phys. Stat. Sol. (a) **203,** 802 (2006).
4. M. A. Green, J. Zhao, A. Wang, P. J. Reece, and M. Gal, Nature **412,** 805 (2001).
5. W. L. Ng, M. A. Lourenco, R. M. Gwilliam, S. Ledain, G. Shao, and K. P. Homewood, Nature **410,** 192 (2001).
6. M. A. Lourenco, M. Milosavljević, G. Shao, R. M. Gwilliam, and K. P. Homewood, Thin Solid Films **504,** 36 (2006).
7. J. M. Sun, T. Dekorsy, W. Skorupa, B. Schmidt, and M. Helm, Appl. Phys. Lett. **83,** 3885 (2003).
8. J. M. Sun, T. Dekorsy, W. Skorupa, B. Schmidt, A. Mücklich, and M. Helm, Phys. Rev. B **70,** 155316 (2004).
9. M. S. Bresler, O. B. Gusev, B. P. Zakharchenya, and I. N. Yassievich, Phys. Sol. State **46,** 5 (2004).
10. N. A. Sobolev, A. M. Emel'yanov, E. I. Shek, and V. I. Vdovin, Phys. B **340-342,** 1031 (2003).
11. V. Kveder, M. Badylevich, E. Steinman, A. Izotov, M. Seibt, and W. Schröter, Appl. Phys. Lett. **84,** 2106 (2004).
12. A. M. Emel'yanov, Yu. A. Nikolaev, N. A. Sobolev, and T. M. Mel'nikova, Semiconductors **38,** 610 (2004).
13. T. Hoang, P. LeMinh, J. Holleman, and J. Schmitz, IEEE Electron Device Lett. **27,** 105 (2006).
14. T. Hoang, J. Holleman, P. LeMinh, J. Schmitz, T. Mchedlidze, T. Arguirov, and M. Kittler, IEEE Trans. Electron Devices **54,** 1860 (2007).
15. P. Y. Yu and M. Cardona, *Fundamentals of Semiconductors* (3rd edn.) (Springer, Berlin, 2001).
16. T. Wada, K. Yasuda, S. Ikuta, M. Takeda, and H. Masuda, J. Appl. Phys. **48,** 2145 (1977).
17. H. J. Queisser, J. Appl. Phys. **32,** 1776 (1961).
18. S. Prussin, J. Appl. Phys. **32,** 1876 (1961).
19. G. H. Schwuttke and H. J. Queisser, J. Appl. Phys. **33,** 1540 (1962).
20. J. J. Lander, H. Schreiber, Jr., T. M. Buck, and J. R. Mathews, Appl. Phys. Lett. **3,** 206 (1963).
21. R. J. Jaccodine, Appl. Phys. Lett. **4,** 114 (1964).
22. M. Kittler, X. Yu, T. Mchedlidze, T. Arguirov, O. F. Vyvenko, W. Seifert, M. Reiche, T. Wilhelm, M. Seibt, O. Voβ, A. Wolff, and W. Fritzsche, Small **3,** 964 (2007).
23. J. Bao, M. Tabbal, T. Kim, S. Charnvanichborikarn, J. S. Williams, M. J. Aziz, and F. Capasso, Opt. Express **15,** 6727 (2007).